3. R. B. Silverman, *Mechanism-Based Enzyme Inactivation: Chemistry and Enzymology* (CRC Press, Boca Raton, FL, 1988).
4. M. C. Findlay, L. C. Dickinson, J. C. W. Chien, *J. Am. Chem. Soc.* **99**, 5168 (1977).
5. G. Moore *et al.*, *J. Inorg. Biochem.* **12**, 1 (1980).
6. Preparative procedures have been described: ZnCcP (*7–10*), ZnCc (*11*), and CuCc (*4*). The ET kinetics were performed by laser flash kinetic spectrophotometry (*7–10*) with the 532-nm output of a Q-switched Nd:yttrium-aluminum-garnet laser under anaerobic conditions at pH 7.0 and 20° ± 0.2°C. The transient absorption apparatus has a transient digitizer (LeCroy) that collects 50,000 data points so that the full progress curve of the intermediate could be collected in a single trace. Before analysis, data were compressed logarithmically. The decays of the ^{3}ZnCcP and ^{3}ZnCc were monitored at 475 nm and 460 nm, respectively. The formation and decay of the resulting charge-transfer intermediate, [(ZnCcP)$^+$, Fe^{2+}Cc], was monitored at a wavelength of 549 nm, the isosbestic point for the ^{3}ZnCcP-ZnCcP absorbance.
7. E. D. A. Stemp and B. M. Hoffman, *Biochemistry* **32**, 10848 (1993).
8. B. M. Hoffman, M. J. Natan, J. M. Nocek, S. A. Wallin, *Struct. Bonding (Berlin)* **75**, 85 (1991).
9. S. A. Wallin *et al.*, *J. Am. Chem. Soc.* **113**, 1842 (1991).
10. J. M. Nocek *et al.*, *ibid.*, p. 6822.
11. J. M. Vanderkooi and M. Erecinska, *Eur. J. Biochem.* **60**, 199 (1975); *ibid.* **64**, 381 (1976).
12. J. S. Zhou and B. M. Hoffman, *J. Am. Chem. Soc.* **115**, 11008 (1993).
13. H. Anni, J. M. Vanderkooi, L. Mayne, *Biochemistry* **34**, 5744 (1995).
14. C. H. Kang, S. Ferguson-Miller, E. Margoliash, *J. Biol. Chem.* **252**, 919 (1977).
15. G. McLendon *et al.*, *J. Am. Chem. Soc.* **115**, 3665 (1993); Q. Zhang *et al.*, *Mol. Cryst. Liq. Cryst.* **199**, 343 (1991).
16. J. S. Zhou and B. M. Hoffman, *Science* **265**, 1693 (1994).
17. M. R. Mauk, J. C. Ferrer, A. G. Mauk, *Biochemistry* **33**, 12609 (1994).
18. The quenching rate constant (k_q) is the difference between the observed (k_{obs}) and the intrinsic (k_D) decay rate constant of ^{3}(ZnCcP).
19. The decay of the ^{3}(ZnCcP) is exponential in the absence and presence of Fe^{3+}Cc. We have ruled out the possibility of a very fast ET process from ^{3}(ZnCcP) to Fe^{3+}Cc by monitoring triplet decay on the microsecond and nanosecond time scales and by observing the lack of an effect of the quencher on the change in the absorbance (ΔA) of ^{3}(ZnCcP) at time zero. This exponential decay behavior of ^{3}ZnCcP indicates that the ET quenching process is in the rapid-exchange limit, that is, the intracomplex ET rate constant is much slower than the complex dissociation rate constant.
20. The effects increase with increasing protein concentrations, but high optical absorbance precludes the use of still higher concentrations.
21. In fact, a quenching titration of ZnCc with Fe^{3+}CcP under these conditions displayed a maximum of k_q = 25 s^{-1} at a concentration ratio of [ZnCc] to [Fe^{3+}CcP] = 2:1; the quenching rate constant decreased with further addition of the quencher Fe^{3+}CcP (*12*).
22. B. M. Hoffman and M. A. Ratner, *J. Am. Chem. Soc.* **109**, 6237 (1987).
23. D. W. Dixon, X. Hong, S. E. Woehler, *Biophys. J.* **56**, 339 (1989).
24. At this point, we are concerned not with the uniqueness of this description but rather with the complexity of the time course. The function explored here is

$$\Delta A = \beta\Sigma\{f_i[\exp(-k_{obs}t) - \exp(-k_it)]/(k_i - k_{obs})\}$$

where k_{obs} is the triplet decay constant, k_i is the thermal back-ET rate constant of phase i, and Σf_i = 1. We are preparing a mechanistic analysis of curves such as those in Fig. 3 (J. S. Zhou, J. M. Nocek, M. L. DeVan, B. M. Hoffman, unpublished results).
25. D. N. Beratan, J. N. Onuchic, J. R. Winkler, H. B. Gray, *Science* **258**, 1740 (1992).
26. C. C. Moser, J. M. Keske, K. Warncke, R. S. Farid, P. L. Dutton, *Nature* **355**, 796 (1992).
27. R. Q. Liu, S. Hahm, M. Miller, B. Durham, F. Millet, *Biochemistry* **34**, 973 (1995).
28. H. Pelletier and J. Kraut, *Science* **258**, 1748 (1992).
29. Indeed, it has been reported that Cc binds to the reaction center at two sites, much as reported here [C. C. Moser and P. L. Dutton, *Biochemistry* **27**, 2450 (1988)].
30. J. S. Zhou and N. M. Kostić, *J. Am. Chem. Soc.* **115**, 10796 (1993); L. Qin and N. M. Kostić, *Biochemistry* **32**, 6073 (1992); I. J. Chang, H. B. Gray, J. R. Winkler, *J. Am. Chem. Soc.* **113**, 7056 (1991).
31. W. B. Church, J. M. Guss, J. J. Potter, H. C. Freeman, *J. Biol. Chem.* **261**, 234 (1986); H. R. R. Engeseth, D. R. McMillin, J. D. Otvos, *ibid.* **259**, 4822 (1984); L. M. Utschig, J. G. Wright, T. V. O'Halloran, *Methods Enzymol.* **226**, 71 (1993).

32. This research was supported under National Institutes of Health grant HL13531.

21 February 1995; accepted 22 May 1995

Experimental Studies and Theoretical Predictions for the H + D_2 → HD + D Reaction

L. Schnieder,* K. Seekamp-Rahn, J. Borkowski, E. Wrede, K. H. Welge, F. J. Aoiz, L. Bañares, M. J. D'Mello, V. J. Herrero, V. Sáez Rábanos, R. E. Wyatt

The H + H_2 exchange reaction constitutes an excellent benchmark with which to test dynamical theories against experiments. The H + D_2 (vibrational quantum number v = 0, rotational quantum number j = 0) reaction has been studied in crossed molecular beams at a collision energy of 1.28 electron volts, with the use of the technique of Rydberg atom time-of-flight spectroscopy. The experimental resolution achieved permits the determination of fully rovibrational state–resolved differential cross sections. The high-resolution data allow a detailed assessment of the applicability and quality of quasi-classical trajectory (QCT) and quantum mechanical (QM) calculations. The experimental results are in excellent agreement with the QM results and in slightly worse agreement with the QCT results. This theoretical reproduction of the experimental data was achieved without explicit consideration of geometric phase effects.

The H + H_2 exchange reaction has been the prototype in the realm of reaction dynamics since the first studies in the field. A good survey of work up to 1990 can be found in (*1*). Particularly intense activity has taken place during the last decade. Great improvements in the quantum dynamical methodology (*2–7*) together with the introduction of laser techniques (*1*) have produced a large amount of new data in a short time, and this rapid progress has not always been free of controversy. The long discrepancy between experiment and theory about the value of the rate constant for the D + H_2 (v = 1) reaction (*1*), the dispute about the possible observation of dynamical resonances in the integral cross section (*1–3, 8, 9*) (finally settled against this possibility), and the tentative assignment of features in the differential cross section to broad QM resonances (*10*), which were later also obtained in a QCT calculation (*11*), are examples of such controversies.

Zare and co-workers (*12–14*) have recently measured rotationally state-specific integral cross sections and rate constants for the D + H_2 (v = 1) → HD (v', j') + H reaction. In a first experiment, they generated D atoms by photolyzing DBr and used resonance-enhanced multiphoton ionization to detect the HD molecules. Noticeable discrepancies were found between the experimental results and several accurate QM (*15*) and QCT (*15*) calculations on different ab initio potential energy surfaces (PESs) (*16, 17*). Further experiments were carried out with DI (*13, 14*), after some experimental problems were detected with the DBr precursor. These measurements were in much better agreement with QCT results (*18*), and especially with new QM calculations (*14*). However, some discrepancies persisted between experiment and theory; these were tentatively attributed to failures in the PES (*14*).

Most theoretical calculations have been carried out on the lowest lying Born-Oppenheimer PES of H_3. In recent works, Kuppermann and Wu (*7*) have shown that a geo-

L. Schnieder, K. Seekamp-Rahn, J. Borkowski, E. Wrede, K. H. Welge, Fakultät für Physik, Universität Bielefeld, Postfach 100131, 33501 Bielefeld, Germany.
F. J. Aoiz and L. Bañares, Departamento de Química Física, Facultad de Química, Universidad Complutense, 28040 Madrid, Spain.
M. J. D'Mello, 4155 National Center for Supercomputing Application, Beckman Institute, 405 North Mathew Avenue, Urbana, IL 61801, USA.
V. J. Herrero, Instituto de Estructura de la Materia, Consejo Superior de Investigaciones Cientificas, Serrano 123, 28006 Madrid, Spain.
V. Sáez Rábanos, Departamento de Química General y Bioquímica, ETS Ingenieros de Montes, Universidad Politécnica, 28040 Madrid, Spain.
R. E. Wyatt, Department of Chemistry and Biochemistry, University of Texas, Austin, TX 78712, USA.

*To whom correspondence should be addressed.

metric phase (GP) effect, associated with the presence of a conical intersection between the two first-adiabatic PESs, might be relevant for the dynamics, especially at relatively high energies. The consideration of the GP effect in accurate QM calculations (*7*) led to excellent agreement with the D + H_2 (v = 1) experiments of Zare and co-workers (*12–14*), including the controversial DBr experiment (*12*). According to these results, GP effects should become gradually noticeable as the energy of the experiment approaches that of the conical intersection between the two PESs (at a total energy E = 2.7 eV). The investigators concluded that the effect had little influence on integral cross sections at values of E lower than about 1.6 eV; however, some differences between GP and non-GP calculations of rotationally resolved differential cross sections (DCSs) were obtained for D + H_2 (v = 0) at E = 1.25 eV (*7*). Unfortunately, the resolution of the existing data for this reaction at this energy, from a crossed-beam experiment by Lee and co-workers (*19*), is too low to allow an interpretation in terms of GP effects. The theoretical prediction (*7*) was that GP effects would become noticeable once fully rotationally resolved experiments were performed.

Recently, Kitsopoulos *et al.* (*20*) applied a novel reaction product imaging technique to the study of H + D_2 (v = 0), which provides an angle-velocity polar map of the reactive scattering in a direct and pictorial way. The experiment was performed at collision energies E_{col} of 0.54 and 1.29 eV (corresponding to total energies of 0.73 and 1.48 eV, respectively). The resolution in this version of the experiment was, however, moderate; it did not allow the identification of vibrational states, and the inverse Abel transformation used to reconstruct the three-dimensional angle-velocity polar map could introduce intensity errors near the symmetry axis, that is, at center-of-mass (CM) scattering angles close to 0° and 180° (*20*). There were some discrepancies between the results of this experiment and the results of QM (*21*, *22*) and QCT (*22*, *23*) calculations, both in the angular and in the velocity distributions of the D atoms, especially at E_{col} = 1.29 eV. The noninclusion of GP effects in the theoretical calculations was invoked as a possible cause of this discrepancy (*24*), and in fact, in a very recent work (*25*), Wu and Kuppermann have performed calculations considering this effect that lead to a much better agreement with the total DCSs of Kitsopoulos *et al.* (*20*). Nevertheless, the D atom time-of-flight (TOF) spectra from an experiment by Welge and co-workers (*26*) with vibrational-state resolution carried out for the H + D_2 (v = 0) reaction at the same energies and based on a Rydberg atom detection technique could be successfully accounted for by both QCT and QM calculations without inclusion of the GP effect (*22*).

From the above considerations, it is clear that the experimental resolution needs to be increased to provide data for a precise and unambiguous comparison with the theoretical predictions of state-to-state cross sections. We report here a much improved version of the last mentioned experiment carried out at the University of Bielefeld, together with a detailed comparison of the measurements with accurate QM and with QCT calculations. The present data, with a well-defined collision and internal energy in the reagents and with rotational-state resolution at each scattering angle, represent, to our knowledge, the highest resolution results available and thus the most stringent test of the quantum theory of reactive scattering. The comparison with QCT results is of practical interest (given the higher flexibility and computational efficiency of the QCT approach as compared with accurate QM methods) and also has conceptual importance, because it can help to assess the adequacy of classical mechanics for the description of nuclear motion during reactive collisions.

The experimental setup (Fig. 1) consists essentially of two parallel pulsed molecular beams, one of *ortho*-D_2 and the other of HI. The *ortho*-D_2 was adiabatically cooled to the ground rotational level j = 0 in a pulsed supersonic expansion from a liquid N_2–cooled reservoir, with basically no contribution from other rotational states (≤2%). Both beams were skimmed into the scattering and detection chamber, where kinematically hot H atoms are produced by the photolysis of HI molecules with linearly polarized fourth-harmonic light of a pulsed Nd:yttrium-aluminum-garnet laser at 266 nm. According to the two spin-orbit components of the halogen atom, two velocity groups of H atoms with spatial distributions perpendicular to each other are produced in the dissociation process. Using 266-nm light, we obtained collision energies of 0.53 and 1.28 eV by directing either the "slow" or the "fast" H atoms toward the D_2 molecular beam; we were able to do this by polarizing the dissociation light either parallel or perpendicular with respect to the desired atomic velocity vector. The collision energy is 10 meV less than in other experiments on H + D_2 where H atoms from the 266-nm photodissociation of HI are used because the speed of the D_2 molecules is reduced to ≈1060 m/s by the expansion of the gas from a cooled reservoir. The estimated spread of the collision energy for the 1.28-eV results is ±5 meV. The velocity distribution of product D atoms is measured according to the technique of Rydberg atom TOF spectroscopy, which was developed at the University of Bielefeld (*27*).

This technique makes use of the high detection efficiency (≈1) and good temporal and spatial resolution achieved by resonantly exciting the product atoms with pulsed laser radiation (time Δt ≈ 5 to 7 ns) into metastable Rydberg states right in the scattering zone

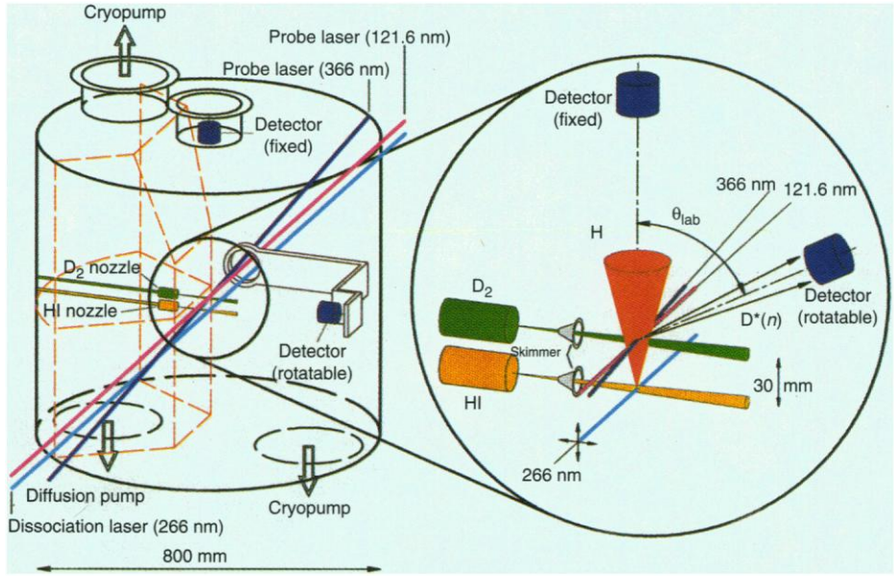

Fig. 1. Schematic view of the experimental setup. The enlargement at right shows a detailed view of the scattering region and detectors. Two parallel pulsed molecular beams, one of *ortho*-D_2 and the other of HI, are skimmed into the scattering and detection chamber. Hot H atoms are produced by the photolysis of the HI molecules with a polarized 266-nm laser. We detected the product D atoms by 1+1 excitation into metastable Rydberg states, using two laser beams of 121.6 and 366 nm. At the end of the drift region, the Rydberg atoms are field-ionized and detected with a particle multiplier.

$$D(1s) + h\nu(121.6\ nm) \rightarrow D^*(2p)$$
$$+ h\nu(366\ nm) \rightarrow D^{**}(n)$$

where h is Planck's constant and ν is the frequency of light. At the end of the drift region, the Rydberg atoms are field-ionized, and the deuterons are detected with a particle multiplier. As the TOF measurement is carried out on neutral atoms, small electric fields may be used to remove any spurious ions produced by the intense laser beams from the flight path, thus increasing the signal-to-noise ratio. Therefore, no differential pumping for the detector is necessary. With a drift path length of 305 mm, the energy resolution ($\Delta E/E$) of the TOF measurement itself is ≈0.5%; this is better by at least a factor of 2 than the overall kinetic energy spread in the product atoms because of the velocity and angular spread of the molecular beams and the angle of acceptance of the detector. The total resolution of the kinetic energy is sufficient to resolve nearly all rovibrational states of the product HD molecule. Given the high detection efficiency, the angle of acceptance for the detector was chosen to be 1° in the plane of the molecular beams and 4° in the plane perpendicular to it.

Theoretical calculations, both classical and QM, have been performed on the Liu-Siegbahn-Truhlar-Horowitz (LSTH) (*16*) PES for the conditions relevant to the experiment just described. These calculations do not explicitly include any GP effect. We calculated converged QM state-to-state integral and differential cross sections for the H + D_2 ($v = 0, j = 0$) → HD + D reaction at the experimental collision energies, using the logarithmic derivative Kohn variational principle, as formulated by Manolopoulos *et al.* (*5*), along with a basis set contraction procedure that significantly improves the efficiency of the calculations (*6*). The convergence of the integral and differential cross sections was carefully monitored as a function of the total angular momentum J. At E_{col} = 1.29 eV, the integral cross sections required the inclusion of the lowest 28 partial waves for a convergence level of better than 0.1% in all cases. The DCS, on the other hand, required the total J sum to run from 0 to 32 in order to yield values stable to within 2% for all angles and all transitions. Details are given in (*22*).

The QCT calculations have been performed on the same PES and for the same conditions as the QM ones. A total number of 2.5×10^5 trajectories were run at this collision energy and initial $j = 0$. The stratified sampling method was used to sample the impact parameter, whose maximum value, b_{max}, was chosen to be 1.3 Å, ensuring that no reaction occurs beyond this value. For the assignment of product quantum numbers, the classical HD molecule rotational angular momentum is equated to $[j'(j' + 1)]^{1/2}\hbar$. With the (real) j' value so obtained, the vibrational quantum number v' is found by equating the internal energy of the outgoing molecule to a Dunham expansion in v', j'. The values of v' and j' found in this way are then rounded to the nearest integer. The rovibrationally resolved DCSs were calculated by the method of moments expansion in Legendre polynomials. A detailed account of the method can be found in (*11, 22, 23*) and references therein.

In order to perform a rigorous comparison between experiment and theory, we have directly simulated the actual laboratory measurements from the theoretical CM DCSs. The procedure used for these simulations is described in (*22*). Figures 2 and 3 show the results for E_{col} = 1.28 eV. Similar data are also available for E_{col} = 0.53 eV; we have chosen to present only the higher energy results here because they are more relevant to the discussion about the GP effect. The degree of agreement between experiment and theory is comparable at both energies.

The experimental kinetic energy spectra of D atoms at three different laboratory scattering angles θ for E_{col} = 1.28 eV (E = 1.47 eV) are shown in Fig. 2, together with the simulation of these measurements based on present QCT and QM results. The resolution of the experiment allows the separation of basically every rovibrational state of the HD product molecule at different values of θ. At the lowest θ, which corresponds to backward HD CM scattering angles, the internal energy distribution is fairly cold, whereas at higher values of θ, which corresponds to decreasing values of the HD CM scattering angle, the distribution becomes rotationally hotter. Experimental scattering data (*20, 26*), with only vibrational-state resolution (*26*), were satisfactorily reproduced with both theoretical approaches. With the present higher resolution measurements, one can distinguish between the QM and QCT results; whereas the QM simulation of the experiment agrees almost perfectly with the measurements, the QCT simulation provides a quite good global description of the experimental data but in some cases fails to reproduce the relative peak intensities and yields slightly hotter rotational distributions than the experimental and QM ones. The same tendency has been observed in earlier comparisons of integral QCT cross sections with QM and experimental results (*6, 15, 22, 23, 28, 29*).

There is also very good agreement between experiment and theory in the variation of the relative total signal with θ. This is shown in Fig. 3, where the experimental and theoretical laboratory angular distributions at E_{col} = 1.28 eV are depicted. During the simulation procedure, we observed that the resulting laboratory angular distributions were very sensitive to the shape of the theoretical total CM DCS. In fact, with somewhat different total CM DCS, as those reported in (*20*), it would not be possible to reproduce the present experimental laboratory angular distribution.

Interestingly, the recent GP calculations of Wu and Kuppermann (*25*) at a collision energy of 1.29 eV (slightly different from the value used in the present experiments) yielded significantly different rotationally resolved DCSs than those of the present

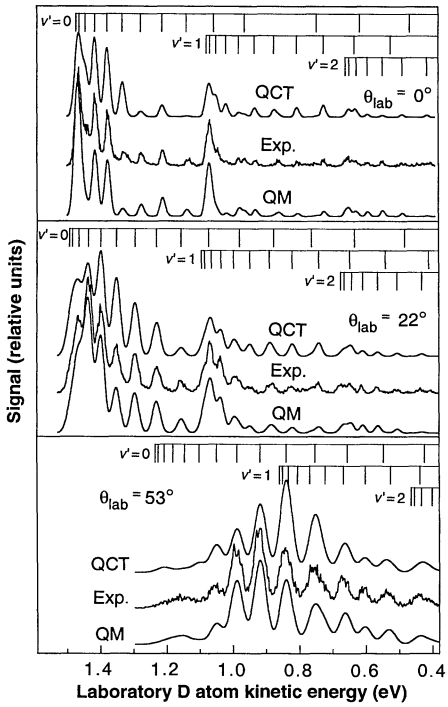

Fig. 2. Laboratory D atom kinetic energy spectra at the indicated laboratory scattering angles θ_{lab} for the H + D_2 ($v = 0, j = 0$) reaction at a collision energy of 1.28 eV. The experimental data are shown along with the QM and QCT theoretical simulations.

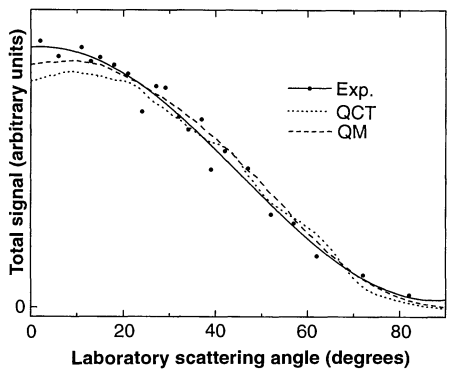

Fig. 3. Total laboratory angular distribution for the H + D_2 ($v = 0, j = 0$) reaction at a collision energy of 1.28 eV. A Legendre polynomial was fitted to the experimental points.

work and could not reproduce the relative heights in the rotational TOF peaks experimentally observed at $E_{col} = 1.28$ eV.

Our data demonstrate that the theoretical results, especially the accurate QM ones, on the reactive scattering of H + D_2 ($v = 0, j = 0$) are essentially correct even at the high level of resolution now obtained. Moreover, the QCT approach seems to provide a very good description of scattering angular distributions to the level of vibrational resolution of the products but leads to some differences when individual rotational states can be resolved. No refinements in the ab initio LSTH PES (*16*) seem necessary, at least for the energies of the experiment. This work shows that the present experimental results at $E_{col} = 1.28$ eV ($E = 1.47$ eV) and under the specified conditions can be explained without explicit consideration of the GP effect.

REFERENCES AND NOTES

1. H. Buchenau, J. P. Toennies, J. Arnold, J. Wolfrum, *Ber. Bunsenges. Phys. Chem.* **94**, 1231 (1990).
2. W. H. Miller, *Annu. Rev. Phys. Chem.* **41**, 245 (1990); J. Z. H. Zhang and W. H. Miller, *Chem. Phys. Lett.* **153**, 465 (1988); *ibid.* **159**, 130 (1989); *J. Chem. Phys.* **91**, 1528 (1989).
3. M. Mladenovic *et al.*, *J. Phys. Chem.* **92**, 7035 (1988); M. Zhao, D. G. Truhlar, N. C. Blais, D. W. Schwenke, D. J. Kouri, *ibid.* **94**, 6696 (1990); D. G. Truhlar, D. W. Schwenke, D. J. Kouri, *ibid.*, p. 7346.
4. R. T. Pack and G. A. Parker, *J. Chem. Phys.* **87**, 3888 (1987); *ibid.* **90**, 3511 (1989); J. D. Kress, Z. Bacic, G. A. Parker, R. T. Pack, *Chem. Phys. Lett.* **157**, 585 (1989); *ibid.* **170**, 306 (1990).
5. D. E. Manolopoulos and R. E. Wyatt, *Chem. Phys. Lett.* **152**, 23 (1988); D. E. Manolopoulos, M. J. D'Mello, R. E. Wyatt, *J. Chem. Phys.* **91**, 6096 (1989).
6. D. E. Manolopoulos, M. J. D'Mello, R. E. Wyatt, *J. Chem. Phys.* **93**, 403 (1990); M. J. D'Mello, D. E. Manolopoulos, R. E. Wyatt, *Chem. Phys. Lett.* **168**, 113 (1990); D. E. Manolopoulos, M. J. D'Mello, R. E. Wyatt, R. B. Walker, *ibid.* **169**, 482 (1990); M. J. D'Mello, D. E. Manolopoulos, R. E. Wyatt, *J. Chem. Phys.* **94**, 5985 (1991).
7. Y. M. Wu, B. Lepetit, A. Kuppermann, *Chem. Phys. Lett.* **186**, 319 (1991); Y. M. Wu and A. Kuppermann, *ibid.* **201**, 178 (1993); A. Kuppermann and Y. M. Wu, *ibid.* **205**, 577 (1993); *ibid.* **213**, 636 (1993).
8. J. C. Nieh and J. J. Valentini, *Phys. Rev. Lett.* **60**, 519 (1988); D. L. Phillips, H. B. Levene, J. J. Valentini, *J. Chem. Phys.* **90**, 1600 (1989).
9. D. A. V. Kliner, D. E. Adelman, R. N. Zare, *J. Chem. Phys.* **94**, 1069 (1991).
10. R. E. Continetti, J. Z. H. Zhang, W. H. Miller, *ibid.* **93**, 5356 (1990); W. H. Miller and J. Z. H. Zhang, *J. Phys. Chem.* **95**, 7767 (1991).
11. F. J. Aoiz, V. J. Herrero, V. Sáez Rábanos, *J. Chem. Phys.* **97**, 7423 (1992).
12. D. A. V. Kliner, D. E. Adelman, R. N. Zare, *ibid.* **95**, 1648 (1991).
13. D. E. Adelman, N. E. Shafer, D. A. V. Kliner, R. N. Zare, *ibid.* **97**, 7323 (1992).
14. D. Neuhauser *et al.*, *Science* **257**, 519 (1992).
15. N. C. Blais, M. Zhao, D. G. Truhlar, D. W. Schwenke, D. J. Kouri, *Chem. Phys. Lett.* **166**, 368 (1990); *ibid.* **188**, 368 (1992); S. L. Mielke, R. S. Friedman, D. G. Truhlar, D. W. Schwenke, D. J. Kouri, *ibid.*, p. 359; W. J. Keogh *et al.*, *ibid.* **195**, 144 (1992).
16. P. Siegbahn and B. Liu, *J. Chem. Phys.* **68**, 2457 (1978); D. G. Truhlar and C. J. Horowitz, *ibid.*, p. 2466; *ibid.* **71**, 1514 (1979).
17. A. J. C. Varandas, F. B. Brown, C. A. Mead, D. G. Truhlar, B. C. Garrett, *ibid.* **86**, 6258 (1987); A. I. Boothroyd, W. J. Keogh, P. G. Martin, M. R. Peterson, *ibid.* **95**, 4343 (1991).
18. F. J. Aoiz, H. K. Buchenau, V. J. Herrero, V. Sáez Rábanos, *ibid.* **100**, 2789 (1994).
19. R. E. Continetti, B. A. Balko, Y. T. Lee, *ibid.* **93**, 5719 (1990).
20. T. N. Kitsopoulos, M. A. Buntine, D. P. Baldwin, R. N. Zare, D. W. Chandler, *Science* **260**, 1605 (1993).
21. S. L. Mielke, D. G. Truhlar, D. W. Schwenke, *J. Phys. Chem.* **98**, 1053 (1994).
22. F. J. Aoiz *et al.*, *J. Chem. Phys.* **101**, 5781 (1994).
23. F. J. Aoiz, V. J. Herrero, O. Puentedura, V. Sáez Rábanos, *Chem. Phys. Lett.* **198**, 321 (1992).
24. M. J. D'Mello, D. E. Manolopoulos, R. E. Wyatt, *Science* **263**, 102 (1994).
25. Y. M. Wu and A. Kuppermann, *Chem. Phys. Lett.* **235**, 105 (1995).
26. L. Schnieder, K. Seekamp-Rahn, F. Liedecker H. Steuwe, K. H. Welge, *Faraday Disc. Chem. Soc.* **91**, 259 (1991).
27. L. Schnieder, W. Meier, K. H. Welge, M. N. R. Ashfold, C. M. Western, *J. Chem. Phys.* **92**, 7027 (1990).
28. N. C. Blais and D. G. Truhlar, *Chem. Phys. Lett.* **102**, 120 (1983); *J. Chem. Phys.* **83**, 2201 (1985).
29. K.-D. Rinnen, D. A. Kliner, R. N. Zare, *J. Chem. Phys.* **91**, 7514 (1989).

30. The experimental part of this project was financed by the German Science Foundation under grants WE 386/19 and SCHN 435/3 and by the Deutscher Akademischer Austauschdienst (Acciones Integradas) 322-AI-e-dr. The Spanish contribution was financed by the Direccion General de Investigacion Cientifica Tecnologica of Spain under grant PB92-0219-C03 and the German-Spanish Scientific Exchange Program "Acciones Integradas" under grants HA-074, HA-113, and HA-135. Research at the University of Texas was supported by the Robert Welch Foundation and the National Science Foundation.

7 March 1995; accepted 3 May 1995

Climate Records Covering the Last Deglaciation

Todd Sowers* and Michael Bender

The oxygen-18/oxygen-16 ratio of molecular oxygen trapped in ice cores provides a time-stratigraphic marker for transferring the absolute chronology for the Greenland Ice Sheet Project (GISP) II ice core to the Vostok and Byrd ice cores in Antarctica. Comparison of the climate records from these cores suggests that, near the beginning of the last deglaciation, warming in Antarctica began approximately 3000 years before the onset of the warm Bølling period in Greenland. Atmospheric carbon dioxide and methane concentrations began to rise 2000 to 3000 years before the warming began in Greenland and must have contributed to deglaciation and warming of temperate and boreal regions in the Northern Hemisphere.

During the late Pleistocene, Earth's climate fluctuated between glacial and interglacial conditions with a period of ~100,000 years. Although changes in Earth's orbit clearly pace climate change, the rapid destruction of the continental ice sheets at the end of a glacial period is not solely the result of simple orbital forcing on the mass balance of the ice sheets. Other factors, such as changes in meridional heat transport by oceans and atmosphere, eustatic sea level rise, changing albedo, and increases in the greenhouse gas concentration, are likely contributors (*1*).

One requirement for understanding the dynamics of a glacial termination is to delineate the sequence of events that characterize it. Here we focus on two elements of the most recent glacial termination: surface temperature records from Greenland and Antarctica and changes in the concentration of greenhouse gases in the atmosphere. We utilize records of the $\delta^{18}O$ of atmospheric O_2 from three ice cores as time stratigraphic markers to transfer the GISP II (central Greenland) varve chronology (*2*, *3*) to the Byrd (West Antarctic) and Vostok (East Antarctic) ice cores. We then compare various ice core climate records with each other as well as with marine and terrestrial climate records and summarize the sequence of events during the last glacial termination.

Records of variations in the $\delta^{18}O$ of atmospheric O_2 with time are based on analyses of trapped gases in several ice cores (*4*, *5*) (Fig. 1A). One can compute $\delta^{18}O_{atm}$ from the measured $\delta^{18}O$ of trapped O_2 after correcting for gravitational fractionation using the $\delta^{15}N$ of trapped N_2 (*6*–*8*). The general nature of the $\delta^{18}O_{atm}$ record from the GISP II, Byrd, and Vostok ice cores is similar: low values throughout the Holocene with a minimum at about 10,000 years ago (10 ka); maximum glacial values that are up to 1.3 per mil higher than at present; and intermediate values during marine isotope stage 3. The major factor influencing the $\delta^{18}O$ of atmospheric O_2 during the past 135,000 years was variability in the $\delta^{18}O$ of seawater resulting from variations in the size of the continental ice sheets (*5*). Secondary factors include variable isotope fractionation associated with respiration, evapotranspiration, and the global hydrologic cycle (*9*). At any one time, $\delta^{18}O_{atm}$ is constant throughout the atmosphere because the time for turnover of atmospheric O_2 [~1200 years (*9*)] is long relative to the interhemispheric

Graduate School of Oceanography, University of Rhode Island, Narragansett, RI 02882, USA.

*Present address: Lamont-Doherty Earth Observatory, Palisades, NY 10964, USA.